

Adaptive Modulation Systems for Predicted Wireless Channels

Sorour Falahati, Arne Svensson, *Fellow, IEEE*,
Torbjörn Ekman and Mikael Sternad *Senior Member, IEEE*

Abstract

When adaptive modulation is used to counter short-term fading in mobile radio channels, signaling delays create problems with outdated channel state information. The use of channel power prediction will improve the performance of the link adaptation. It is then of interest to take the quality of these predictions into account explicitly when designing an adaptive modulation scheme. We study the optimum design of an adaptive modulation scheme based on uncoded M-QAM modulation assisted by channel prediction for the flat Rayleigh fading channel. The data rate, and in some variants the transmit power, are adapted to maximize the spectral efficiency subject to average power and bit error rate constraints. The key issues studied here are how a known prediction error variance will affect the optimized transmission properties such as the SNR boundaries that determine when to apply different modulation rates, and to what extent it affects the spectral efficiency. This investigation is performed by analytical optimization of the link adaptation, using the statistical properties of a particular but efficient channel power predictor. Optimum solutions for the rate and transmit power are derived based on the predicted SNR and the prediction error variance.

keywords: flat Rayleigh fading channels, adaptive modulation, channel prediction

1 Introduction

Spectrally efficient communication techniques are of great importance in future wireless communications. Adaptive modulation, or link adaptation, is a powerful technique for improving the spectral efficiency in wireless transmission over fading channels. If complete Channel State Information (CSI) is known at the transmitter, the Shannon capacity of a fading channel can be approached by optimal adaptation of the signaling parameters such as transmit power, data rate, channel coding rate or scheme [1,2]. Adaptive modulation has been extensively studied in [3–14] and the references therein.

With adaptive modulation, a high spectral efficiency is attainable at a given Bit Error Rate (BER) in favorable channel conditions, while a reduction of the throughput is experienced when the channel degrades. The adaptation can also take requirements of different traffic classes and services such as required BERs, into account.

We consider *fast* link adaptation, i.e. we strive to adapt to the small scale fading. The receiver estimates the received power and sends feedback information via a return channel to the transmitter, with the aim of modifying the modulation parameters. Due to the unavoidable delays involved in power estimation, feedback transmission and modulation adjustment, estimates of the CSI will be based on outdated information. In the so far proposed solutions for optimum design of adaptive modulation systems, perfect knowledge of the CSI at the transmitter as well as error free channel estimates at the receiver are common assumptions for the system design and performance evaluation. In real systems, these assumptions are not valid. Due to the time-varying nature of wireless channels, the channel status will change during the time delay between estimation and data transmission. This leads to performance degradation such as decrease in the throughput.

The impact of the uncertainty in channel estimates on the performance has been discussed in the literature (see e.g. [5–7, 15–21]). In [17], the effect of channel estimation errors on the BER performance is illustrated. However, this effect is investigated on the receiver side,

not on the choice of link adaptation parameters. In [5, 6], the impact of time delay on the adaptive modulation performance is characterized. It is shown that systems with low BER requirements are very sensitive to the time delay. They can operate acceptably only if the delay is kept below a critical small value.

The theoretically optimal way of handling the problem would be to optimally estimate the conditional probability density function (pdf) of the BER for a given modulation format, conditioned on all past received signals and other relevant information. The modulation format would then be adjusted based on this pdf. This approach is unfortunately hard to realize, since the BER is a nonlinear function of the channel power gain, which is a quadratic function of the complex channel. We are therefore forced to consider a suboptimal two-step approach: The channel power gain is predicted by a (theoretically sub-optimum) scheme, and the adaptive modulation system is analyzed, and preferably adjusted, based on the statistics of these predictions.

Adaptive modulation based on prediction has been studied in some previous works. In [7], a linear predictor is used to estimate the current channel status based on the outdated estimates. The channel status is used to determine the currently appropriate modulation, and the effect of small time delays and the mobile speed on the BER and throughput performance are studied. However, the Signal-to-Noise Ratio (SNR) thresholds which determine the modulation modes are evaluated based on the simulation results only. Results by Goeckel [15, 16] highlight that to design a practical adaptive modulation system, time variations of the channel which severely degrade the system performance, should be taken into account. There, a novel approach to the design of a robust adaptive modulation system based on only a single outdated fading estimate is proposed. In [18–20], adaptive modulation schemes based on long-range CSI predictions that assume the use of perfect channel estimates, are investigated. A channel predictor based on Pilot Symbol Assisted Modulation (PSAM) is developed in [21] where the impact of the prediction error on the system performance is analyzed.

The system proposed here utilizes an unbiased quadratic regression of past noisy channel estimates to predict the signal power at the receiver. This algorithm is developed and analyzed in [22, 23]. This predictor is not claimed to be optimal, but from our experience it produces the best performance on measured data among all known channel power predictions, if it uses smoothed noise-reduced complex channel estimates as regressors. Also, closed-form expressions exist for the prediction error statistics when the predictor is applied to Rayleigh fading channels. Starting from the major assumption that the second-order statistics of the channel is known, these expressions will be used in this paper for optimizing the rate adaptation scheme and for analyzing the resulting BER and spectral efficiency for given prediction error variances.

We restrict our attention to link adaptation with uncoded M-QAM modulation. With no coding, the two remaining degrees of freedom are the choice of modulation formats in different SNR regions, and the possibility to use transmit power control within these regions. Exploitation of the statistical information about the prediction errors will be shown to improve the overall system performance, and adjusts the link adaptation better to the true channel conditions. As a result, the BER constraints will be fulfilled also in the presence of prediction errors. This will not be the case if the prediction errors are neglected in the design of the link adaptation. It turns out to be quite important to take into account the prediction errors that are realistically encountered in long-range prediction (by 0.1-0.5 wavelengths) of flat Rayleigh fading channels. Also, low rate region boundaries that are active in fading dips, will be shown to be affected much more by the prediction error than higher rate boundaries.

This paper is organized as follows. Section 2 describes the system model and the notations which are used throughout this study. The channel prediction is explained in Section 3. The BER is evaluated as a function of predicted instantaneous SNR in Section 4 and optimal rate and power adaptation are derived under different constraints in Section 5. Analytical results are presented in Section 6 while Section 7 summarizes the results.

2 System Model

In the adaptive modulation, M-QAM modulation schemes with different constellation sizes are provided at the transmitter. For each transmission, the modulation scheme and possibly also the transmit power are adjusted to maximize the spectral efficiency, under BER and average power constraints, based on the instantaneous predicted SNR. The channel is modeled by a flat Rayleigh fading channel. At the receiver, demodulation is performed using channel estimates. The discrete model of the system is depicted in Figure 1. All the signals are sampled at the symbol rate where the index n represents the signal sample at time nT_s where T_s is the symbol period. Here, g_n is the zero mean, complex channel gain with circular Gaussian distribution where the power $|g_n|^2$ is $\chi^2(2)$, or exponentially distributed. The auto-correlation function of the complex channel gain is denoted by

$$r_g(m) = E(g_n g_{n-m}^*). \quad (1)$$

In the following, r_g will denote the average channel power gain $E|g_n|^2 = r_g(0)$. Moreover, w_n is a sample from a complex white Gaussian noise process, with zero mean and time-invariant variance σ_w^2 . The estimate y_{n-L} is the noisy observation of g_{n-L} at the receiver, obtained by a pilot-aided channel estimator that does not need to be specified in detail in this context. The delay L is the prediction horizon and is assumed to be long enough to take the computational and signaling delays in the adaptation control loop into account. A time-series of these estimates is used at the receiver to predict the channel power gain $|g_n|^2$ which is proportional to the instantaneous received SNR, denoted by γ_n . The appropriate rate and transmission power levels are fed back to the transmitter where an error free feed-back channel is assumed. In practice, the feedback information is quantized to limit the return channel bandwidth. This added source of error is not taken into account in the analysis.

Based on the predicted SNR denoted by $\hat{\gamma}_{n|n-L}$ or $\hat{\gamma}$, a modulation scheme with con-

stellation size $M(\hat{\gamma})$ (out of N constellations available at the transmitter), which transmits $k(\hat{\gamma}) = \log_2 M(\hat{\gamma})$ bits per symbol, and a transmit power $S(\hat{\gamma})$ are selected. Each block of $k(\hat{\gamma})$ data bits denoted by \mathbf{b}_n , is Gray encoded and mapped to a symbol in the signal constellation denoted by s_n , which is transmitted over the flat Rayleigh fading channel. The received sample, r_n , is used to estimate the channel gain \tilde{g}_n , which in turn is used to detect the transmitted bits denoted by $\hat{\mathbf{b}}_n$. Since the estimation error in \tilde{g}_n is believed to have a minor effect on the performance compared to the prediction error, perfect channel estimation is here assumed for the coherent demodulation.

In this study, the following notations similar to those of [14] are used. Let \bar{S} denote the average transmit signal power. The average received SNR is then given by

$$\bar{\gamma} = r_g \frac{\bar{S}}{\sigma_w^2}. \quad (2)$$

For a constant transmit power \bar{S} , the instantaneous received SNR is

$$\gamma_n = \bar{\gamma} \frac{p_n}{r_g} \quad (3)$$

where $p_n = |g_n|^2$ is the instantaneous channel power gain. Correspondingly, the instantaneous predicted received SNR is

$$\hat{\gamma} = \hat{\gamma}_{n|n-L} = \bar{\gamma} \frac{\hat{p}_{n|n-L}}{r_g} \quad (4)$$

where $\hat{p}_{n|n-L}$ is the predicted instantaneous channel power gain $|g_n|^2$. For the transmit power $S(\hat{\gamma})$, the instantaneous received SNR is given by $\gamma_n(S(\hat{\gamma})/\bar{S})$, with γ_n given by (3).

The rate region boundaries, defined as the ranges of $\hat{\gamma}$ values over which the different constellations are used by the transmitter, are denoted by $\{\hat{\gamma}_i\}_{i=0}^{N-1}$. When the predicted instantaneous SNR belongs to a given rate region, i.e. $\hat{\gamma} \in [\hat{\gamma}_i, \hat{\gamma}_{i+1})$, the corresponding constellation of size $M(\hat{\gamma}) = M_i$ with $k(\hat{\gamma}) = k_i$ bits per symbol is transmitted where $\hat{\gamma}_N = \infty$. There is no transmission if $\hat{\gamma} < \hat{\gamma}_0$, meaning that $\hat{\gamma}_0$ is the cutoff SNR.

3 Channel Prediction

The absolute square, i.e. the power, of the time series g_n is to be predicted based on the observations y_n that are assumed to be affected by an additive estimation error e_n . Thus, $y_n = g_n + e_n$. The channel estimator which produces y_n is assumed to be unbiased and to operate linearly on the received baseband signal. A reasonable assumption on e_n , used in the following, is that it is a zero mean complex circular Gaussian random variable which is independent of g_n . Based on a finite number of past observations of y_n , the complex channel at time n is predicted with a prediction horizon L by a linear FIR filter

$$\hat{g}_{n|n-L} = \varphi_{n-L}^H \theta \quad (5)$$

where θ is a column vector containing K complex-valued predictor coefficients and

$$\varphi_{n-L}^H = [y_{n-L}, y_{n-L-m}, \dots, y_{n-L-(K-1)m}], \quad (6)$$

is the regressor vector where H represents a Hermitian transpose. A Wiener adjustment of θ provides the optimal linear predictor in the Mean Square Error (MSE) sense.

To provide the best prediction performance on fading channels for a limited pre-specified number K of parameters, the delay spacing m (the time delay between consecutive channel samples in the regressor) should be selected in a way appropriate for the fading rate. The predictor performance will be improved by the use of good channel estimates within (6), obtained by the application of noise-reducing smoothing [22–24].

The adjustment of an adaptive modulation scheme is determined not by the complex channel gain g_n , but by the SNR at the time of transmission. If we, for simplicity, assume that the variance of the noise and disturbance w_n in Figure 1 is constant, the channel power $p_n = |g_n|^2$ will have to be predicted. However, the use of the squared magnitude of the linear prediction $\hat{g}_{n|n-L}$ as a predictor of the channel power would on average underestimate the true power, and result in a biased estimate. The reason is that the predictability of g_n

decreases with L . The average power of $\hat{g}_{n|n-L}$ will therefore decrease with an increasing prediction horizon L and be lower than the average power of g_n . We here instead utilize a recently developed quadratic power predictor [22] which eliminates this bias and enables the attainment of a lower power estimation MSE. It is constructed by adding the true average power r_g and subtracting $E(|\hat{g}_{n|n-L}|^2)$ from the estimate $|\hat{g}_{n|n-L}|^2$:

$$\hat{p}_{n|n-L} = \theta^H \varphi_{n-L} \varphi_{n-L}^H \theta + r_g - \theta^H \mathbf{R}_\varphi \theta. \quad (7)$$

Here, $\mathbf{R}_\varphi = E(\varphi_{n-L} \varphi_{n-L}^H)$ is the $K \times K$ correlation matrix for the regressors. Note that $E(\hat{p}_{n|n-L}) = r_g$ for all L . The unbiased quadratic predictor that minimizes the power MSE is derived in [22], assuming second-order statistics of g_n to be known. It is shown there that the predictor coefficient vector θ that provides an MSE optimal the channel predictor (5) will *also* result in an MSE optimal power predictor, when used in (7). The optimal adjustment for both of these problems is thus given by

$$\theta = \mathbf{R}_\varphi^{-1} \mathbf{r}_{g\varphi}, \quad (8)$$

$$\mathbf{r}_{g\varphi} = E\{g_n \varphi_{n-L}\} = [r_g(L), r_g(L+m), \dots, r_g(L+(K-1)m)]^T. \quad (9)$$

If θ is perfectly adjusted, the minimum mean square value of the channel gain prediction error $\epsilon_{c_n} = g_n - \hat{g}_{n|n-L}$ and the power prediction error $\epsilon_{p_n} = p_n - \hat{p}_{n|n-L}$ will be given by

$$\sigma_{\epsilon_c}^2 = r_g - \mathbf{r}_{g\varphi}^H \mathbf{R}_\varphi^{-1} \mathbf{r}_{g\varphi}, \quad (10)$$

$$\sigma_{\epsilon_p}^2 = r_g^2 - |\mathbf{r}_{g\varphi}^H \mathbf{R}_\varphi^{-1} \mathbf{r}_{g\varphi}|^2, \quad (11)$$

respectively. Thus, by (8) and (7), the optimum unbiased quadratic power prediction can be expressed in terms of the MSE-optimal linear FIR channel prediction as

$$\hat{p}_{n|n-L} = |\hat{g}_{n|n-L}|^2 + \sigma_{\epsilon_c}^2. \quad (12)$$

In other words, the squared magnitude of the optimal FIR channel prediction (5), with θ by (8), is modified simply by adding the variance (10) of the channel estimate. The bias compensation will reduce the total prediction MSE. It also provides superior performance as compared to the use of linear power predictors that are based on channel power samples ($|y_n|^2$) as regressors [23]. For a given prediction $\hat{p}_{n|n-L}$ by (12), the conditional power prediction error variance, denoted by $\sigma_{\epsilon_p}^2|\hat{p}_{n|n-L}$, is given by (eq. (7.48) in [23])

$$\sigma_{\epsilon_p}^2|\hat{p}_{n|n-L} = \sigma_{\epsilon_c}^2[2\hat{p}_{n|n-L} - \sigma_{\epsilon_c}^2]. \quad (13)$$

If we average over the predicted power in (13), we obtain

$$\sigma_{\epsilon_p}^2 = \sigma_{\epsilon_c}^2[2r_g - \sigma_{\epsilon_c}^2], \quad (14)$$

since, with the unbiased predictor, $E(\hat{p}_{n|n-L}) = E(p_n) = r_g$ (This expression can also be obtained by substituting (10) into (11)).

An important indication of the predictor performance is the *relative* standard deviation of the conditional power prediction error. Using (13), this measure is given by

$$\frac{\sigma_{\epsilon_p}|\hat{p}_{n|n-L}}{\hat{p}_{n|n-L}} = \sigma_{\epsilon_c}\sqrt{\frac{2\hat{p}_{n|n-L} - \sigma_{\epsilon_c}^2}{\hat{p}_{n|n-L}}}. \quad (15)$$

For a given σ_{ϵ_c} , (15) increases as $\hat{p}_{n|n-L}$ becomes small, i.e. when we predict a fading dip.

To solve the rate adaptation optimization problem, the pdf of the instantaneous SNR is required. In section 8 of [23], it is shown that if an unbiased quadratic power predictor with optimized parameters, is used which provides a given $\sigma_{\epsilon_c}^2/r_g$, then the pdf of γ_n conditioned

on $\hat{\gamma}_{n|n-L}$ will be given by

$$f_{\gamma}(\gamma|\hat{\gamma}) = \frac{U(\gamma)U(\hat{\gamma} - \bar{\gamma}\sigma_{\epsilon_c}^2/r_g)}{\bar{\gamma}\sigma_{\epsilon_c}^2/r_g} \exp \left[-\frac{\gamma + \hat{\gamma} - \bar{\gamma}\sigma_{\epsilon_c}^2/r_g}{\bar{\gamma}\sigma_{\epsilon_c}^2/r_g} \right] I_0 \left(\frac{2}{\bar{\gamma}\sigma_{\epsilon_c}^2/r_g} \sqrt{\gamma(\hat{\gamma} - \bar{\gamma}\sigma_{\epsilon_c}^2/r_g)} \right), \quad (16)$$

where $U(\cdot)$ is the Heaviside's step function, $\bar{\gamma}$ is given by (2) and $I_0(\cdot)$ is the zeroth order modified Bessel function. The time index n was dropped in the pdf expressions since γ_n and $\hat{\gamma}_{n|n-L}$ are both stationary random processes. The pdf of $\hat{\gamma}$ will be given by

$$f_{\hat{\gamma}}(\hat{\gamma}) = \frac{U(\hat{\gamma} - \bar{\gamma}\sigma_{\epsilon_c}^2/r_g)}{\bar{\gamma}(1 - \sigma_{\epsilon_c}^2/r_g)} \exp \left[-\frac{\hat{\gamma} - \bar{\gamma}\sigma_{\epsilon_c}^2/r_g}{\bar{\gamma}(1 - \sigma_{\epsilon_c}^2/r_g)} \right]. \quad (17)$$

This is a shifted $\chi^2(2)$ -distribution, with the shift $\bar{\gamma}\sigma_{\epsilon_c}^2/r_g$ caused by the bias compensation term in (7) and (12).

4 M-QAM BER Performance

The transmitter adjusts the constellation size and possibly also the transmit power based on the instantaneous predicted SNR $\hat{\gamma}_{n|n-L}$, where the time index n will be dropped in the following. Evaluation of the optimal power and constellation size (or rate) adjustments which maximize the spectral efficiency and satisfy the BER requirement, requires an invertible expression for the BER as a function of $\hat{\gamma}$. Assuming a square M-QAM with Gray encoded bits, constellation size M_i , and transmit power $S(\hat{\gamma})$, the instantaneous BER as a function of γ and $\hat{\gamma}$ on an Additive White Gaussian Noise (AWGN) channel, is approximated by [14]

$$\text{BER}(\gamma, \hat{\gamma}) \approx 0.2 \exp \left(\frac{-1.6\gamma}{M_i - 1} \frac{S(\hat{\gamma})}{\bar{S}} \right) \quad (18)$$

which is tight within 1 dB for $M_i \geq 4$ and $\text{BER} \leq 10^{-3}$. Moreover, the instantaneous BER as a function of the instantaneous predicted SNR¹, $\hat{\gamma}$, is obtained as

¹This is an average over the pdf over the true instantaneous SNR for one specific modulation scheme.

$$\text{BER}(\hat{\gamma}) = \int_0^\infty \text{BER}(\gamma, \hat{\gamma}) f_\gamma(\gamma|\hat{\gamma}) d\gamma. \quad (19)$$

Using (16) to average (18) over the whole range of the instantaneous true SNR, γ , results in

$$\text{BER}(\hat{\gamma}) \approx 0.2z(\hat{\gamma}) \exp [(1 - x(\hat{\gamma}))(1 - z(\hat{\gamma}))] \quad (20)$$

where

$$x(\hat{\gamma}) = \frac{\hat{\gamma}}{\bar{\gamma}\sigma_{\epsilon_c}^2/r_g}, \quad (21)$$

$$z(\hat{\gamma}) = \frac{1}{1 + A_i S(\hat{\gamma})}, \quad (22)$$

$$A_i = \frac{1.6}{M_i - 1} \frac{\bar{\gamma}\sigma_{\epsilon_c}^2/r_g}{\bar{S}}. \quad (23)$$

Note that $x(\hat{\gamma}) \geq 1$ since $\hat{\gamma} \geq \bar{\gamma}\sigma_{\epsilon_c}^2/r_g$ by (17) and that $0 \leq z(\hat{\gamma}) < 1$. Finally, similar to [14], the average BER is given by

$$\overline{\text{BER}} = \frac{\sum_{i=0}^{N-1} k_i \int_{\hat{\gamma}_i}^{\hat{\gamma}_{i+1}} \text{BER}(\hat{\gamma}) f_{\hat{\gamma}}(\hat{\gamma}) d\hat{\gamma}}{\sum_{i=0}^{N-1} k_i \int_{\hat{\gamma}_i}^{\hat{\gamma}_{i+1}} f_{\hat{\gamma}}(\hat{\gamma}) d\hat{\gamma}}. \quad (24)$$

In [25], it is shown that the use of (18) which gives the analytical expression (20) for the instantaneous BER, results in a small approximation error as compared to integrating (8) in [14] (which is a more accurate approximation for BER) in (19).

5 Optimal Rate and Power Adaptation

The spectral efficiency of a modulation scheme is given by the average data rate per unit bandwidth (R/B) where R is the data rate and B is the transmitted signal bandwidth. When a modulation with constellation size M_i is chosen, the instantaneous data rate is k_i/T_s [bps].

Assuming the Nyquist data pulses ($B = 1/T_s$), the spectral efficiency is given by

The term *instantaneous* BER refers to the fact that the BER is a function of instantaneous predicted SNR.

$$\bar{\eta} = \sum_{i=0}^{N-1} k_i \int_{\hat{\gamma}_i}^{\hat{\gamma}_{i+1}} f_{\hat{\gamma}}(\hat{\gamma}) d\hat{\gamma} \quad \text{bps/Hz.} \quad (25)$$

As explained in Section 2, a transmission rate is assigned to each rate region boundary. The rate region boundaries will be adjusted to maximize the spectral efficiency, subject to various constraints. For SNR levels between the rate boundaries, the transmit power may furthermore be adjusted. We thus have an optimization problem with two possible degrees of freedom: the rate region boundaries and the transmit power.

In this work, we consider the following scenarios. First, we intend to maximize the spectral efficiency where both the average power and instantaneous BER are constrained. The transmit power as well as the rate are adapted to satisfy the requirements. Then, we study a case where constant transmit power is presumed. The motivation is that the data rate adaptation has the major effect in increasing the spectral efficiency as compared to the power adaptation, as shown by [5,12]. Also, transmission with variable power complicates the practical implementation: transmission of only integers k_i requires less feedback bandwidth as compared to using fast adaptive modulation combined with fast power control. We thereafter relax the BER constraint by constraining the average BER (24) instead of the instantaneous BER (19), which results in an increase in the spectral efficiency.

We illustrate the derivation of the optimum rate region boundaries and possibly also transmit power adjustment of these cases. Once the optimal rate region boundaries are evaluated, the spectral efficiency can easily be obtained according to (25).

5.1 Instantaneous BER and variable power (I-BER, V-Pow)

The case we consider first is maximizing the spectral efficiency subject to the average transmit power constraint

$$\int_0^{\infty} S(\hat{\gamma}) f_{\hat{\gamma}}(\hat{\gamma}) d\hat{\gamma} \leq \bar{S} \quad (26)$$

and the instantaneous BER constraint

$$\text{BER}(\hat{\gamma}) = \text{TBER} \quad (27)$$

where TBER denotes the target BER. The constraint (27) together with (20) show that one of the variables, i.e. $z(\hat{\gamma})$ or $x(\hat{\gamma})$, can be expressed in terms of the other one. Hence, we take the natural logarithm of (27) based on (20) and then use the Taylor approximation $\ln z(\hat{\gamma}) \approx z(\hat{\gamma}) - 1$ about $z(\hat{\gamma}) = 1$ to obtain

$$z(\hat{\gamma}) \approx 1 - \frac{1}{x(\hat{\gamma})} \ln(0.2/\text{TBER}). \quad (28)$$

By substituting (21) and (22) in the above equation, we obtain an expression for the power adjustment within the SNR region for rate i given by

$$S_i(\hat{\gamma}) \approx \left[\frac{\frac{1}{A_i} \frac{\bar{\gamma} \sigma_{\epsilon_c}^2}{r_g} \ln(0.2/\text{TBER})}{\hat{\gamma} - \frac{\bar{\gamma} \sigma_{\epsilon_c}^2}{r_g} \ln(0.2/\text{TBER})} \right] \text{U} \left(\hat{\gamma} - \frac{\bar{\gamma} \sigma_{\epsilon_c}^2}{r_g} \ln(0.2/\text{TBER}) \right) \quad (29)$$

where

$$S_i(\hat{\gamma}) = S(\hat{\gamma}), \quad \hat{\gamma} \in [\hat{\gamma}_i, \hat{\gamma}_{i+1}). \quad (30)$$

Figure 2 compares the transmit power based on (29) to that which is obtained by solving (27) numerically. It is shown that the approximation error in (28) results in negligible errors.

Hence, the optimization problem can be simplified to a search for the optimal rate region boundaries. For this purpose, we form the Langrangian function from the spectral efficiency criterion (25) and the power constraint (26), which is here treated as an equality constraint. It is given by

$$J(\hat{\gamma}_0, \hat{\gamma}_1, \dots, \hat{\gamma}_{N-1}) = \sum_{i=0}^{N-1} k_i \int_{\hat{\gamma}_i}^{\hat{\gamma}_{i+1}} f_{\hat{\gamma}}(\hat{\gamma}) d\hat{\gamma} + \lambda \left(\sum_{i=0}^{N-1} \int_{\hat{\gamma}_i}^{\hat{\gamma}_{i+1}} S_i(\hat{\gamma}) f_{\hat{\gamma}}(\hat{\gamma}) d\hat{\gamma} - \bar{S} \right) \quad (31)$$

where $\lambda \neq 0$ is the Lagrangian multiplier. Solving

$$\frac{\partial J}{\partial \hat{\gamma}_i} = 0, \quad 0 \leq i \leq N - 1 \quad (32)$$

results in

$$S_{i-1}(\hat{\gamma}_i) - S_i(\hat{\gamma}_i) = \frac{k_i - k_{i-1}}{\lambda} \quad 0 \leq i \leq N - 1 \quad (33)$$

where $k_{-1} = 0$ and $S_{-1}(\hat{\gamma}) = 0$. From (29) and (33), we obtain

$$\hat{\gamma}_i = \ln \left(\frac{0.2}{\text{TBER}} \right) \left(\frac{\bar{\gamma} \sigma_{\epsilon_c}^2}{r_g} - \frac{\bar{S}}{1.6} \frac{M_i - M_{i-1}}{k_i - k_{i-1}} \lambda \right), \quad 0 \leq i \leq N - 1. \quad (34)$$

The Lagrange multiplier λ is numerically evaluated based on the power constraint (26).

Given (29) and (34), the average power constraint (26) can be written as

$$\begin{aligned} \sum_{i=0}^{N-1} \int_{\hat{\gamma}_i}^{\hat{\gamma}_{i+1}} S_i(\hat{\gamma}) f_{\hat{\gamma}}(\hat{\gamma}) d\hat{\gamma} &= \rho \exp \left(\frac{\sigma_{\epsilon_c}^2 / r_g}{1 - \sigma_{\epsilon_c}^2 / r_g} (1 - \ln(0.2/\text{TBER})) \right) \times \\ \sum_{i=0}^{N-2} (M_i - 1) (\text{Ei}(\rho \lambda P_i) - \text{Ei}(\rho \lambda P_{i+1})) &+ (M_{N-1} - 1) \text{Ei}(\rho \lambda P_{N-1}) \leq \bar{S} \end{aligned} \quad (35)$$

where $\text{Ei}(\cdot)$ is the Exponential Integral and for convenience, the notations

$$\rho = -\ln \left(\frac{0.2}{\text{TBER}} \right) \frac{\bar{S}}{1.6 \bar{\gamma} (1 - \sigma_{\epsilon_c}^2 / r_g)}, \quad P_i = \frac{M_{i-1} - M_i}{k_{i-1} - k_i}, \quad 0 \leq i \leq N - 1 \quad (36)$$

are used. Here, the average power constraint will be fulfilled if $\lambda < 0$. A *bisection method* is used to numerically search for λ which meets the power constraint with equality.

5.2 Instantaneous BER and constant power (I-BER, C-Pow)

We now consider the use of an instantaneous BER constraint and of a constant transmit power $S(\hat{\gamma}) = S$ that is adjusted to satisfy the average power constraint (26) with equality.

The BER expression (20) then becomes

$$\text{BER}(\hat{\gamma}) = \frac{0.2}{1 + A_i S} \exp \left[\frac{A_i S}{1 + A_i S} (1 - x(\hat{\gamma})) \right]. \quad (37)$$

The average power constraint (26), implies that the cut off SNR $\hat{\gamma}_0$, should satisfy

$$\frac{S}{\bar{S}} = \frac{1}{\int_{\hat{\gamma}_0}^{\infty} f_{\hat{\gamma}}(\hat{\gamma}) d\hat{\gamma}} \quad (38)$$

which implies that the transmit power used when transmission does occur will be higher than \bar{S} , and it is given by

$$S = \bar{S} \exp \left[\frac{\hat{\gamma}_0 - \bar{\gamma} \sigma_{\epsilon_c}^2 / r_g}{\bar{\gamma} (1 - \sigma_{\epsilon_c}^2 / r_g)} \right]. \quad (39)$$

Moreover, the instantaneous BER constraint must be fulfilled at all the rate region boundaries such that

$$\text{BER}(\hat{\gamma}) \leq \text{BER}(\hat{\gamma}_i) = \text{TBER}, \quad \hat{\gamma} \in [\hat{\gamma}_i, \hat{\gamma}_{i+1}), \quad 0 \leq i \leq N - 1 \quad (40)$$

which by (37) and (21) results in

$$\hat{\gamma}_i = \frac{\bar{\gamma} \sigma_{\epsilon_c}^2}{r_g} \left[1 - \frac{1 + A_i S}{A_i S} \ln \left(\frac{\text{TBER}}{0.2} (1 + A_i S) \right) \right], \quad 0 \leq i \leq N - 1. \quad (41)$$

Thus, the cut-off SNR $\hat{\gamma}_0$ and the transmit power S are found through (39) and (41). Once it is done, $\{\hat{\gamma}_i\}_{i=1}^{N-1}$ are easily obtained from (41).

5.3 Average BER and constant power (A-BER, C-Pow)

Finally, we investigate the case concerning the average BER constraint with constant transmit power. Similar to Section 5.2, the transmit power must satisfy (38). The average BER constraint is given by

$$\overline{\text{BER}} \leq \text{TBER}, \quad (42)$$

where (37) is used for the instantaneous BER in (24). Forming the Lagrangian function from the criterion (25) and the constraint (42), here treated as an equality constraint, gives

$$J(\hat{\gamma}_0, \hat{\gamma}_1, \dots, \hat{\gamma}_{N-1}) = \sum_{i=0}^{N-1} k_i \int_{\hat{\gamma}_i}^{\hat{\gamma}_{i+1}} f_{\hat{\gamma}}(\hat{\gamma}) d\hat{\gamma} + \lambda \left(\sum_{i=0}^{N-1} k_i \int_{\hat{\gamma}_i}^{\hat{\gamma}_{i+1}} (\text{BER}(\hat{\gamma}) - \text{TBER}) f_{\hat{\gamma}}(\hat{\gamma}) d\hat{\gamma} \right). \quad (43)$$

The optimum rate region boundaries are found through solving

$$\frac{\partial J}{\partial \hat{\gamma}_i} = 0, \quad 0 \leq i \leq N-1 \quad (44)$$

which results in

$$\text{BER}(\hat{\gamma}_i) = \text{TBER} - \frac{1}{\lambda}, \quad 0 \leq i \leq N-1. \quad (45)$$

Similar to the previous case, we have

$$\hat{\gamma}_i = \frac{\bar{\gamma} \sigma_{\epsilon_c}^2}{r_g} \left[1 - \frac{1 + A_i S}{A_i S} \ln \left(\frac{\text{TBER} - \frac{1}{\lambda} (1 + A_i S)}{0.2} \right) \right], \quad 0 \leq i \leq N-1. \quad (46)$$

We can evaluate the optimal rate region boundaries and transmit power through (39) and (46) based on λ that satisfies the average BER constraint. As shown in Appendix A, the optimal solution that fulfills the average BER constraint with equality exists when $\text{TBER} < \frac{1}{1+A_0 S}$. Otherwise, the solution results in a lower average BER than required with a consequent reduction in the spectral efficiency. For more details, see Appendix A.

6 Results and discussion

We assume that six different M-QAM signal constellations corresponding to 4-QAM, 16-QAM, 64-QAM, 256-QAM, 1024-QAM and 4096-QAM, are available at the transmitter. Although the use of very large constellations is questionable from the practical point of view, it is included here to illustrate the effect of prediction errors of various magnitude.

The results presented here are evaluated for flat Rayleigh fading channels with $r_g = 1$.

The optimal region boundaries for different policies when the required BER² is TBER = 10^{-3} , the prediction error variances are $\sigma_{\epsilon_p}^2 = 0.001$ and 0.1 ³ and the average received SNR is $\bar{\gamma} = 20$ dB, can be seen from Figures 3, 4 and 5. Figure 3 shows that for the *I-BER*, *V-Pow* policy, the transmit power follows the inverse water-filling pattern w.r.t. $\hat{\gamma}$ within each rate region interval. The peak power within each interval increases as the rate increases. Figure 4 illustrates that under *I-BER*, *C-Pow* policy, the instantaneous BER does not exceed the required BER while it reaches the target BER at the boundaries, as intended. Finally, as shown in Figure 5, the *A-BER*, *C-Pow* policy results in an instantaneous BER fluctuation around the required average BER to maintain the target BER on average.

An interesting phenomenon observed in these figures is the effect of the prediction error variance on the SNR thresholds: When a large prediction error variance is taken into account, the boundaries are *raised* for SNRs lower than the average SNR. To a less extent, they are usually *lowered* for SNRs higher than the average SNR. A reasonable explanation is that when we predict into a fading dip (low SNR), the *relative* conditional prediction standard deviation (15) will become larger. This will contribute to making the scheme cautious when entering fading dips. As the prediction error variance is increased, the scheme would not transmit at all during an increasing fraction of the time (when $\hat{\gamma} < \bar{\gamma}$). Due to the average power constraint, this allows the use of higher transmit power when transmission is allowed. For $\hat{\gamma} \gg \bar{\gamma}$, the effect caused by power constraint sometimes dominates which explains why the SNR limits belonging to the large constellation sizes can be reduced.

Figure 6 shows how the average SNR affects some of the rate boundaries of the adaptive

²Corresponding results for TBER = 10^{-7} are available in [25].

³Since $r_g = 1$, $\sigma_{\epsilon_p}^2$ will here represent the normalized power prediction MSE (NMSE). For comparison, the use of the average power r_g as a power prediction would result in a prediction error variance $\sigma_{\epsilon_p}^2 = 0.5$ for all prediction horizons. For a flat fading channel with Jakes spectrum and a SNR in y_n of 20 dB, $\sigma_{\epsilon_p}^2 = 0.1$ corresponds to a prediction 0.3 wavelengths ahead in space, while $\sigma_{\epsilon_p}^2 = 0.01$ is obtained when predicting 0.1 wavelengths ahead [22,23]. The level $\sigma_{\epsilon_p}^2 = 0.001$ is essentially equivalent to perfect prediction of the channel power.

M-QAM schemes for $TBER = 10^{-3}$ and $\sigma_{\epsilon_p}^2 = 0.1$. As observed, the SNR thresholds below the average SNR are increased more than the ones above the average. This effect increases with the prediction error variance as could be seen from Figures 3, 4 and 5. The increase in the rate boundaries is the largest for *I-BER*, *V-Pow* policy, while *A-BER*, *C-Pow* policy shows the least sensitivity.

The maximum spectral efficiency for $TBER = 10^{-3}$ and $\sigma_{\epsilon_p}^2 = 0.001$ and 0.1 are illustrated in Figure 7 for the three considered policies. The features observed in this figure are as follows. The gain in the spectral efficiency when using good predictors is considerable as compared to the poor predictors. Comparing different policies from the spectral efficiency point of view, we see that for small prediction error variance, the highest and lowest spectral efficiencies are provided by *I-BER*, *V-Pow* and *I-BER*, *C-Pow*, respectively due to the highest and lowest degrees of freedom, respectively. However, as the predictor deteriorates, the spectral efficiencies of all the policies become closer to each other.

Finally, Figure 8 is shown to highlight the importance of considering realistic assumptions for the design. In this example, the adaptive modulation systems are designed under the assumption of *perfect channel prediction* at the transmitter. However, the transmitted signals are experiencing different channels than the predicted ones, due to the inaccuracy in the prediction. In other words, the SNR thresholds and transmit power are determined for perfect CSI, while the resulting BER and spectral efficiency are calculated using $f_\gamma(\gamma|\hat{\gamma})$ and $f_{\hat{\gamma}}(\hat{\gamma})$ for erroneous predictions. The results are shown for the channel prediction error variances $\sigma_{\epsilon_p}^2 = 0.001$ and 0.1 and target BER $TBER = 10^{-3}$. The two uppermost figures illustrate the instantaneous BER for the average received SNR $\bar{\gamma} = 20$ dB while the lower figure shows the average BER for $\bar{\gamma} = 10$ to 40 dB. The results indicate that the adaptive scheme based on *I-BER*, *V-Pow* is extremely sensitive to the accuracy of the statistical measures used in the design. If perfect prediction is assumed for the design while the predictor produces seemingly insignificant errors (i.e. $\sigma_{\epsilon_p}^2 = 0.001$), the BER requirement

is no longer satisfied. The reason is that both the rate boundaries and the instantaneous transmit power are affected by these errors and increase the BER considerably (see (20)). The adaptive scheme based on *I-BER*, *C-Pow* and *A-BER*, *C-Pow* policies are less sensitive to small prediction errors (i.e. for $\sigma_{\epsilon_p}^2 = 0.001$) which are neglected in the design and can still attain the target BER. However, it is evident that the target BER will no longer be attained if large prediction errors are not taken into account when adjusting the rate and the transmit power.

7 Conclusion

The optimum design of an adaptive modulation scheme based on uncoded M-QAM modulation is investigated. The transmitter adjusts the transmission rate and possibly also power based on the predicted SNR to maximize the spectral efficiency while satisfying the BER and average transmit power constraints. Optimum solutions for adjusting the adaptive rate and transmit power are derived. The analytical results show that when the prediction error increases, the rate region boundaries for a given constellation size are raised for the SNRs lower than average SNR, while they are sometimes lowered for the SNRs higher than the average SNR. Moreover, the spectral efficiency decreases as the predictor error variance increases. Also, the gain due to the transmission with varying power is minor and becomes even negligible when the prediction quality deteriorates. It is demonstrated that the BER considerably increases when the system is not designed based on realistic assumptions such as erroneous prediction.

The optimization problem that is discussed here, can be solved for any family of modulations, as long as accurate BER expressions (which are invertible and differentiable) in terms of the predicted SNR are available. A competitive candidate is Trellis Coded Modulation (TCM) which will improve the spectral efficiency at a given $\bar{\gamma}$ [26].

A Appendix

Here, we discuss that the optimal rate region boundaries explained in Section 5.3, exist if the search interval for λ is carefully chosen. For simplicity, we denote $\alpha = \frac{\bar{\gamma}\epsilon_c^2}{r_g - \bar{\gamma}\epsilon_c^2}$ and $x(\hat{\gamma}_i) = x_i$ where $x_i \geq 1$. Based on (39) and (46), we have to solve $f(x_i) = 0$ for $i = 0$ where

$$f(x_i) = 1 - x_i - \frac{1 + A_0\bar{S}e^{\alpha(x_0-1)}}{A_0\bar{S}e^{\alpha(x_0-1)}} \ln \left(\frac{\text{TBER} - \frac{1}{\lambda}}{0.2} (1 + A_0\bar{S}e^{\alpha(x_0-1)}) \right). \quad (47)$$

It can be easily shown that $f(x_0)$ is a monotonic function while $x_0 \geq 1$. Since $f(x_0 \rightarrow +\infty) \rightarrow -\infty$, then $f(x_0) = 0$ has a solution if $f(x_0 = 1) \geq 0$. This condition implies that

$$\begin{cases} \text{if } \text{TBER} > \frac{0.2}{1+A_0\bar{S}} & \text{then } 1/\text{TBER} < \lambda < 1/\left(\text{TBER} - \frac{0.2}{1+A_0\bar{S}}\right), \\ \text{if } \text{TBER} < \frac{0.2}{1+A_0\bar{S}} & \text{then } \lambda < 1/\left(\text{TBER} - \frac{0.2}{1+A_0\bar{S}}\right) \text{ or } \lambda > 1/\text{TBER}. \end{cases} \quad (48)$$

Since we aim at $\overline{\text{BER}} = \text{TBER}$, considering that $\text{BER}(\hat{\gamma})$ decreases as $\hat{\gamma}$ increases, the intuition is to have $\text{BER}(\hat{\gamma}_i) > \text{TBER}$ for $0 \leq i \leq N - 1$ which based on (45), implies that $\lambda < 0$. The results from (48) show that this condition is satisfied only for $\lambda \in \Lambda_2$. Therefore, when $\text{TBER} < \frac{0.2}{1+A_0\bar{S}}$, a numerical search based on a *bisection method* for $\lambda \in \Lambda_2$, is used to find a λ which meets the average BER constraint (42) with equality.

Otherwise, when $\text{TBER} > \frac{0.2}{1+A_0\bar{S}}$, we see that by increasing λ , the average BER increases but never reaches to TBER. Therefore, in this case we choose $\lambda = 1/(\text{TBER} - \frac{1}{1+A_0\bar{S}})$ to obtain the closest possible value to the average target BER. By this choice, the rate region boundaries are found through similar procedure as explained in Section 5.2.

References

- [1] A. J. Goldsmith and P. Varaiya, "Capacity of fading channels with channel side information," *IEEE Transactions on Information Theory*, vol. 43, no. 6, pp. 1986–1992, Nov. 1997.
- [2] A. J. Goldsmith, "The capacity of downlink fading channels with variable rate and power," *IEEE Transactions on Vehicular Technology*, vol. 46, no. 3, pp. 569–580, Aug. 1997.
- [3] B. Vucetic, "An adaptive coding scheme for time-varying channels," *IEEE Transactions on Communications*, vol. 39, no. 5, pp. 653–663, May 1991.
- [4] S. M. Alamouti and S. Kallel, "Adaptive trellis-coded multiple-phase-shift keying for Rayleigh fading channels," *IEEE Transactions on Communications*, vol. 42, no. 6, pp. 2305–2314, June 1994.

- [5] M.-S. Alouini and A. J. Goldsmith, "Adaptive M-QAM modulation over Nakagami fading channels," in *IEEE Global Communications Conference*, Phoenix, Arizona, Nov. 1997, pp. 218–223.
- [6] A. J. Goldsmith and S. Chua, "Variable-rate variable-power MQAM for fading channels," *IEEE Transactions on Communications*, vol. 45, no. 10, pp. 1218–1230, Oct. 1997.
- [7] V. K. N. Lau and M. D. MacLeod, "Variable rate adaptive trellis coded QAM for high bandwidth efficiency applications in Rayleigh fading channels," in *Proc. IEEE Vehicular Technology Conference*, May 1998, vol. 1, pp. 348–352.
- [8] A. J. Goldsmith and S. Chua, "Adaptive coded modulation for fading channels," *IEEE Transactions on Communications*, vol. 46, no. 5, pp. 595–602, May 1998.
- [9] T. Ue, S. Sampei, N. Morinaga, and K. Hamaguchi, "Symbol rate and modulation level-controlled adaptive modulation/TDMA/TDD system for high-bit-rate wireless data transmission," *IEEE Transactions on Vehicular Technology*, vol. 47, no. 4, pp. 1134–1147, Nov. 1998.
- [10] M.-S. Alouini, X. Tang, and A. J. Goldsmith, "An adaptive modulation scheme for simultaneous voice and data transmission over fading channels," *IEEE Journal on Selected Areas in Communications*, vol. 17, no. 5, pp. 837–850, May 1999.
- [11] K. J. Hole, H. Holm, and G. E. Øien, "Adaptive multidimensional coded modulation over flat fading channels," *IEEE Journal on Selected Areas in Communications*, vol. 18, no. 7, pp. 1153–1158, July 2000.
- [12] C. Köse and D. L. Goeckel, "On power adaptation in adaptive signaling systems," *IEEE Transactions on Communications*, vol. 48, no. 11, pp. 1769–1773, Nov. 2000.
- [13] V. K. N. Lau and M. D. Macleod, "Variable-rate trellis coded QAM for flat-fading channels," *IEEE Transactions on Communications*, vol. 49, no. 9, pp. 1550–1560, Sept. 2001.
- [14] S. T. Chung and A. J. Goldsmith, "Degrees of freedom in adaptive modulation: a unified view," *IEEE Transactions on Communications*, vol. 49, no. 9, pp. 1561–1571, Sept. 2001.
- [15] D. L. Goeckel, "Robust adaptive coded modulation for time-varying channels with delayed feedback," in *Thirty-Fifth Annual Allerton Conference on Communication, Control, and Computing*, Oct. 1997, pp. 370–379.
- [16] D. L. Goeckel, "Adaptive coding for time-varying channels using outdated fading estimates," *IEEE Transactions on Communications*, vol. 47, no. 6, pp. 844–855, June 1999.
- [17] X. Tang, M.-S. Alouini, and A. J. Goldsmith, "Effect of channel estimation error on M-QAM BER performance in Rayleigh fading," *IEEE Transactions on Communications*, vol. 47, no. 12, pp. 1856–1864, Dec. 1999.
- [18] S. Hu, A. Duel-Hallen, and H. Hallen, "Adaptive modulation using long range prediction for flat Rayleigh fading channels," in *IEEE International Symposium on Information Theory*, Sorrento, Italy, June 25-30 2000, vol. 2, p. 159.
- [19] S. Hu and A. Duel-Hallen, "Combined adaptive modulation and transmitter diversity using long range prediction for flat fading mobile radio channels," in *Global Telecommunications Conference*, San Antonio, Texas, November 25-29 2001, vol. 2, pp. 1256–1261.
- [20] T. S. Yang and A. Duel-Hallen, "Adaptive modulation using outdated samples of another fading channel," in *Wireless Communications and Networking Conference*, Orlando, Florida, USA, March 17-21 2002, pp. 477–481.
- [21] G. E. Øien, H. Holm, and K. J. Hole, "Channel prediction for adaptive coded modulation in Rayleigh fading," in *European Signal Processing Conference*, Toulouse, France, Sept. 3-6 2002.
- [22] T. Ekman, M. Sternad, and A. Ahlén, "Unbiased power prediction on broadband channel," in *Proc. IEEE Vehicular Technology Conference*, Vancouver, Canada, Sept. 2002.
- [23] T. Ekman, "Prediction of mobile radio channels, modeling and design," PhD thesis, Signals and Systems, Uppsala University, Uppsala, Sweden. Online: <http://www.signal.uu.se/Publications/abstracts/a023.html>, Oct. 2002.
- [24] M. Sternad, T. Ekman, and A. Ahlén, "Power prediction on broadband channels," in *Proc. IEEE Vehicular Technology Conference*, Rhodes, Greece, May 2001.
- [25] S. Falahati, "Adaptive modulation and coding in wireless communications with feedback," PhD thesis, Signals and Systems, Chalmers University of Technology, Göteborg, Sweden, <http://www.s2.chalmers.se/publications/>, Oct. 2002.
- [26] S. Falahati, A. Svensson, M. Sternad, and H. Mei, "Adaptive trellis-coded modulation over predicted flat fading channels," in *Proc. IEEE Vehicular Technology Conference*, Orlando, Florida, USA, Oct. 2003.

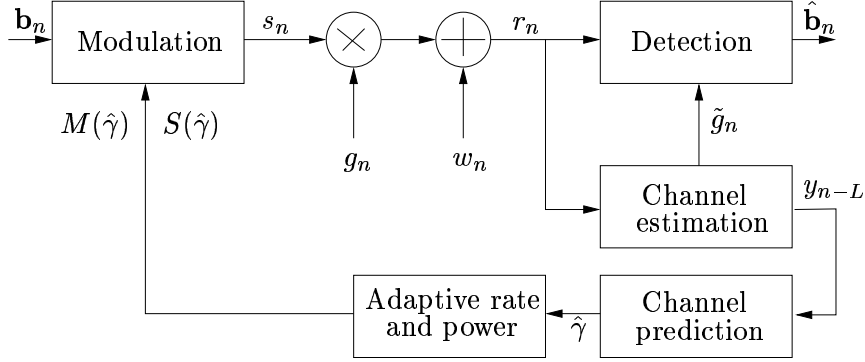


Figure 1: Discrete model of the system.

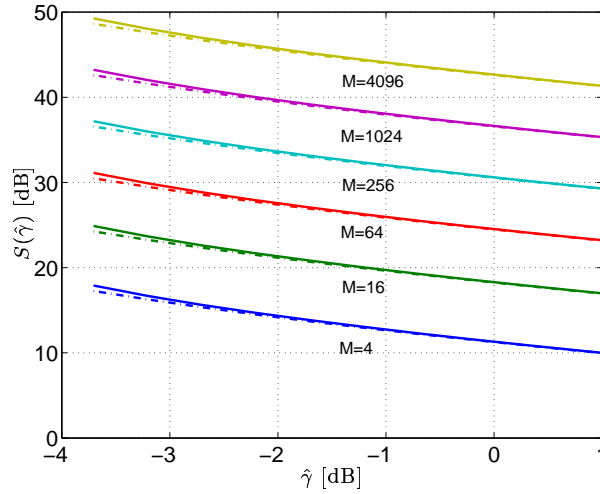


Figure 2: Optimum transmit power versus instantaneous predicted SNR. The solid lines correspond to the solution obtained from (29) using the Taylor approximation and the dashed-dotted lines correspond to the numerical solution of (27). The results are shown for different constellation sizes M , $\bar{\gamma} = 20$ dB, $\text{TBER} = 10^{-3}$ and $\sigma_{\epsilon_p}^2 = 0.001$.

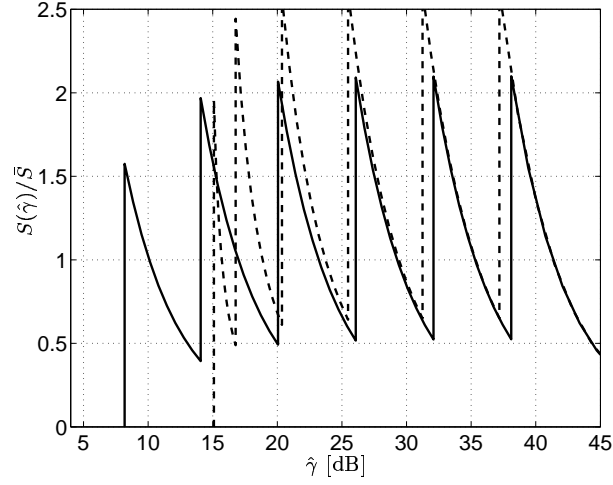


Figure 3: *I-BER, V-Pow* policy: Optimum normalized transmit power versus instantaneous predicted SNR of M-QAM schemes for $\bar{\gamma} = 20$ dB and TBER = 10^{-3} . The solid and dashed lines correspond to $\sigma_{\epsilon_p}^2 = 0.001$ and 0.1, respectively.

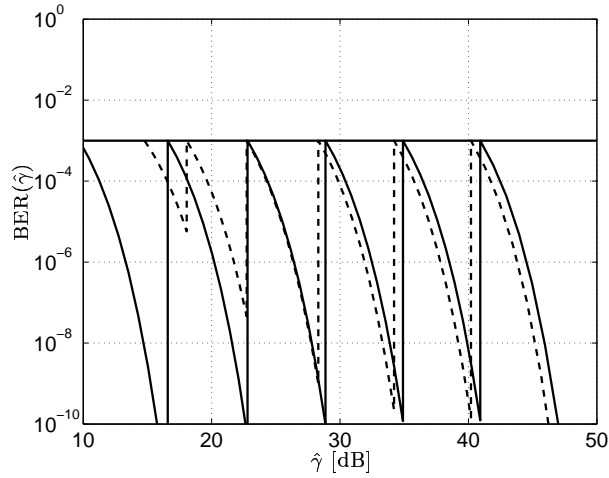


Figure 4: *I-BER, C-Pow* policy: Instantaneous BER versus instantaneous predicted SNR of M-QAM schemes for $\bar{\gamma} = 20$ dB and TBER = 10^{-3} . The solid and dashed lines correspond to $\sigma_{\epsilon_p}^2 = 0.001$ and 0.1, respectively.

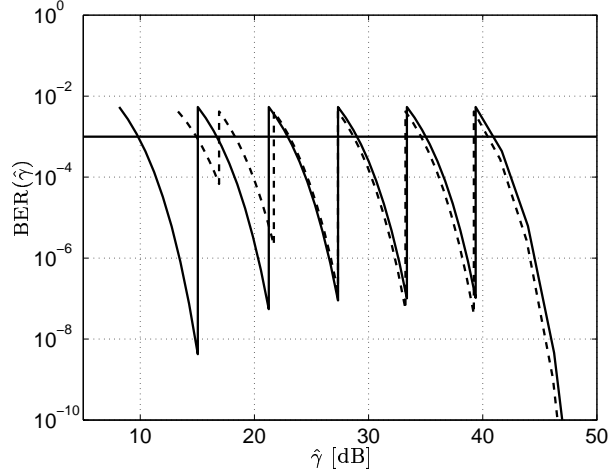


Figure 5: *A-BER, C-Pow* policy: Instantaneous BER versus instantaneous predicted SNR of M-QAM schemes for $\bar{\gamma} = 20$ dB and $TBER = 10^{-3}$. The solid and dashed lines correspond to $\sigma_{\epsilon_p}^2 = 0.001$ and 0.1 , respectively.

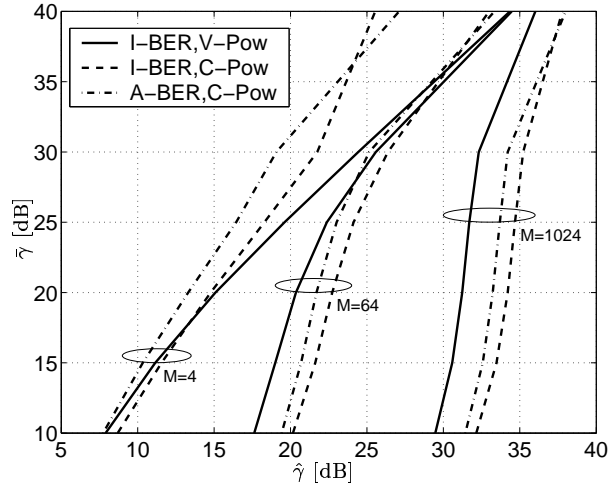


Figure 6: Optimum rate region boundaries of the three considered transmission schemes in terms of the average SNR for $TBER = 10^{-3}$ and $\sigma_{\epsilon_p}^2 = 0.1$.

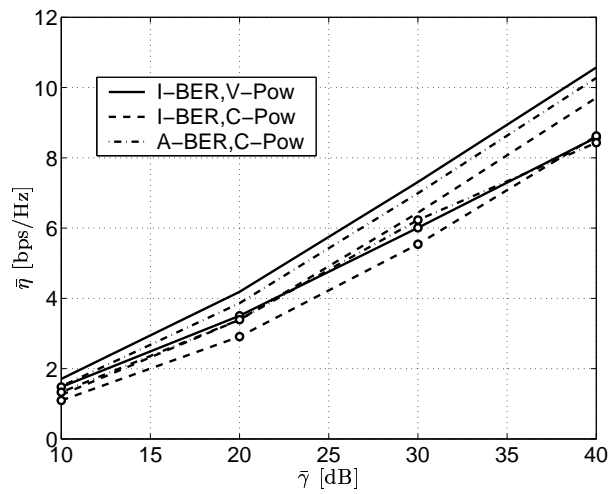


Figure 7: M-QAM Spectral efficiency versus average received SNR for TBER = 10^{-3} for the three policies considered here. The lines with and without rings correspond to $\sigma_{\epsilon_p}^2 = 0.1$ and 0.001, respectively.

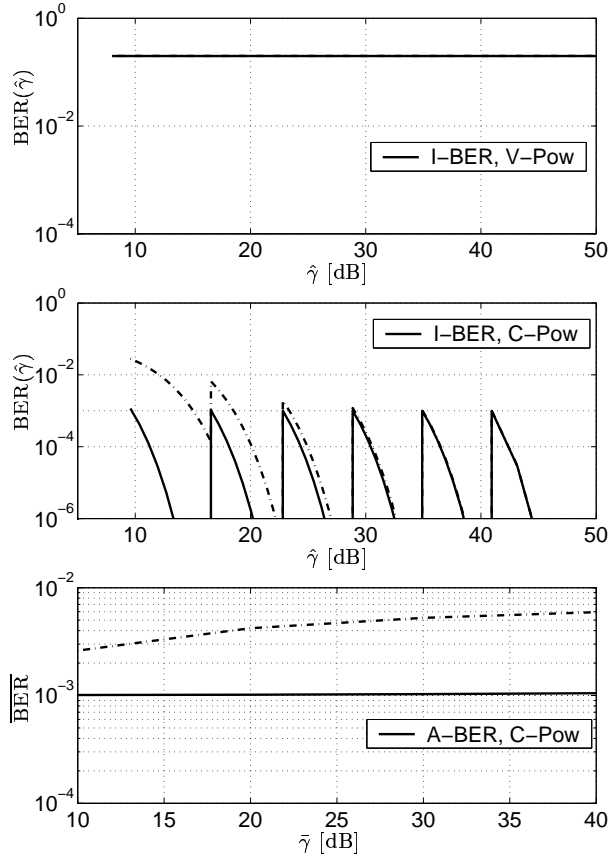


Figure 8: The effect of imperfect CSI on the BER performance of M-QAM schemes. The results are shown for the three considered transmission schemes when the prediction uncertainty is not taken into account in the rate and power adaptation, for a required TBER = 10^{-3} . For the *I-BER*, *V-Pow* and *I-BER*, *C-Pow* policies, $\bar{\gamma} = 20$ dB. The solid and dashed-dotted lines correspond to $\sigma_{\epsilon_p}^2 = 0.001$ and 0.1 , respectively. Note that on the upper plot, the solid and dashed-dotted line overlap.